Full-spectrum fitting method applied to YAG:Dy : Impact of oxygen content and laser fluence on wall-temperature phosphor thermometry for combustion

Tobias Guivarch, Hugo Samson, Jérôme Bonnety, Jessy Elias, Sébastien Ducruix, Clément Mirat, Christopher Betrancourt, Guilhem Dezanneau, Ronan Vicquelin

Full-Spectrum Fitting Method Applied to YAG:Dy : Impact of Oxygen Content and Laser Fluence on Wall-Temperature Phosphor Thermometry for Combustion

Tobias Guivarch[a,*], Hugo Samson[a,*], Jérôme Bonnety[a], Jessy Elias[a], Sébastien Ducruix[a], Clément Mirat[a], Christopher Betrancourt[a], Guilhem Dezanneau[b], Ronan Vicquelin[a]

[a] *Université Paris-Saclay, CNRS, CentraleSupélec, Laboratoire EM2C, Gif-sur-Yvette, France*
[b] *Université Paris-Saclay, CNRS, CentraleSupélec, Laboratoire SPMS, Gif-sur-Yvette, France*

Abstract

Achieving the European net-zero greenhouse gas emissions target requires the development of sustainable combustion processes across various industrial sectors. These promising alternatives introduce new challenges, such as modifying wall heat transfer. Accurate surface temperature measurements are essential for understanding these effects. Laser-Induced Phosphorescence (LIP) provides a semi-invasive method that exploits the temperature-dependent phosphorescence spectra of thermographic phosphors. YAG:Dy is a thermographic phosphor that emits a phosphorescence signal over the range of 300 K to 2000 K. However, its poor sensitivity with the intensity ratio method and its low sensitivity at lower temperatures with the lifetime method limit its use to high-temperature combustion applications. Additionally, its sensitivity to ambient oxygen reduces the accuracy of those methods. This study evaluates the performance of the Full-Spectrum Fitting (FSF) method, developed by the EM2C Laboratory in Lechner et al. (2022), when applied to YAG:Dy. The method leverages the phosphor's spectral temperature dependence over a wide range (303 to 1773 K), achieving an accuracy of 0.3 K and a precision of 8.4 K under given experimental conditions. It is observed that there is a laser fluence threshold above which temperature determination using the FSF method becomes independent of laser fluence. The impact of YAG:Dy's sensitivity to oxygen concentration on temperature measurement is quantified. In the worst case, uncertainty in oxygen concentration can introduce a temperature error ranging from 7 to 19 K. Guidelines are provided to help mitigate these sensitivities in combustion applications.

Keywords: Phosphor Thermometry; Laser Diagnostic; Oxygen effect; Laser Fluence effect; YAG:Dy; FSF method

Information for Editors and Reviewers

1) Novelty and Significance Statement

The novelty of this research is the application of the Full-Spectrum Fitting (FSF) Method — a spectral variant of Laser-Induced Phosphorescence (LIP) — to YAG:Dy thermographic phosphors, specifically examining the influence of oxygen content and laser fluence on the normalized phosphorescence spectra; additionally, X-ray diffraction (DRX) was performed on the YAG:Dy sample to determine its exact crystal structure.
The significance lies in the method's demonstrated accuracy (0.3 K) and precision (8.4 K) across a broad temperature range (303–1773 K) under controlled experimental conditions. Beyond benchmark performance, the investigation provides valuable insights into how laser fluence and oxygen content affect phosphorescence spectra and temperature determination. From these insights, practical guidelines are provided for deploying the FSF method with YAG:Dy in real-world combustion chambers, ensuring reliable thermometry while minimizing temperature determination biases.

2) Author Contributions

- TG : Performing experiments, Designing research, Analyzing data, Writing, Review and Editing.
- HS : Performing experiments, Designing research, Analyzing data, Writing, Review and Editing.
- JB : Performing experiments, Analyzing data, Designing Test bench, Writing, Review and Editing.
- JE : Designing Test bench.
- SD : Review, Editing and Acquiring Fundings.
- CM : Designing research, Analyzing data, Designing Test bench, Writing, Review and Editing.
- CB : Designing research, Analyzing data, Designing Test bench, Writing, Review, Editing and Acquiring Fundings.
- GD : Performing experiments, Designing research, Analyzing data, Review and Editing.
- RV : Designing research, Analyzing data, Writing, Review, Editing and Acquiring Fundings.

1. Introduction

The European Union's ambition to achieve climate neutrality by 2050 necessitates the rapid deployment of technologies capable of attaining net-zero greenhouse gas emissions. Among these, sustainable combustion processes play a crucial role in decarbonizing various industrial sectors, including transportation, energy production, and steam generation. However, promising alternatives to conventional industrial combustion methods present new challenges, such as modifying heat transfer to the walls or the load. For instance, in CH_4 or H_2 oxy-combustion, the high concentration of CO_2 and/or H_2O in the burnt gases significantly impacts heat transfer [1].

Accurate and non-intrusive surface temperature measurements are essential for assessing thermal loads in combustion chambers. Among available methods, Laser-Induced Phosphorescence (LIP) thermometry is a semi-intrusive laser diagnostic technique that leverages the temperature-dependant phosphorescence emissions of luminophore materials (thermographic phosphors). In this method, a phosphorescent coating is applied to the target surface, which, upon laser excitation, emits a phosphorescence signal that correlates with temperatures [1–3]. In the combustion community, for applications such as IC engines or gas turbines, LIP has recently attracted significant interest, beyond its semi-intrusive nature, accuracy, and ability to provide two-dimensional temperature fields [4–6].

To ensure reliable temperature measurements, LIP requires a calibration step in which the phosphorescence signal is recorded at known temperatures. Two main approaches have been developed in the literature [2, 3]: the lifetime method and spectral methods. The lifetime method is based on the temperature-dependant decay time of the phosphorescence signal [7], whereas spectral methods analyze variations in the emission spectrum. Within spectral methods, two techniques exist: the intensity ratio method [8], which evaluates intensity variations at two distinct wavelength bands, and the Full-Spectrum Fitting (FSF) method, a recently developed and applied technique at Laboratory EM2C [9, 10]. The FSF method leverages the entire emission spectrum by fitting its shape, offering improved measurements precision.

Various thermographic phosphors have been used in LIP thermometry, each with specific advantages and limitations [3]. Some phosphors exhibit sensitivity to oxygen concentration in the surrounding atmosphere [7, 11–15], particularly in lifetime-based methods. In combustion applications, and more specifically in oxy-combustion, where oxygen levels fluctuate due to the presence of burned or fresh gases, this sensitivity can introduce measurement and calibration uncertainties. Additionally, some thermographic phosphors display dependencies on laser fluence, which may affect the accuracy of LIP methods [9, 16–18]. Furthermore, different phosphors are suited for different temperature ranges, making the selection of an appropriate thermographic phosphor crucial for reliable measurements [3].

For instance, $Mg_{3.5}FGeO_5$:Mn, which is the only thermographic phosphor tested with the FSF method to date, is known to be insensitive to oxygen concentration [12] but presents spectral sensibility to laser fluence [9] and becomes impractical for measurements above 1000 K due to diminished signal intensity and lifetime [1].

Conversely, $Y_3Al_5O_{12}$:Dy (YAG:Dy) has been widely used in high temperature environments with both intensity ratio and decay time methods at temperature exceeding 1200 K [6, 19–23]. This thermographic phosphor exhibits spectral dependence on temperature and remains detectable at high temperatures, making it a good candidate for the FSF method on a wide range of temperatures. In some studies, no effect of oxygen concentration on YAG:Dy phosphorescence has been observed [11, 21, 24], while others report an influence [7, 15]. In particular, Nilsson et al. [7] observe an increase in lifetime with higher oxygen content, whereas Ishiwada et al. [15] report the opposite. Both have shown that oxygen concentration affects both the lifetime and intensity of YAG:Dy phosphorescence. Despite this, limited information is available on the effect of oxygen concentration [15] and on the impact of laser fluence [18] on the normalized spectra of this thermographic phosphor. Understanding these effects on YAG:Dy phosphorescence spectra is crucial for ensuring the reliability and accuracy of the FSF method.

This study investigates the feasibility of using the FSF method for accurate temperature measurement based on the temperature-dependent spectral dynamics of YAG:Dy. It aims to be applied on industrial-like combustion chambers, where the steady-state temperature is generally reached over the course of several tens of minutes and where temperatures can range from ambient to 1200 K within just a few centimeters [1].

Furthermore, it examines the performance of the FSF method when applied to YAG:Dy, considering both oxygen and laser fluence dependencies.

This article is structured as follows: First, the experimental approach used in this study is presented. Next, the FSF method and its application to YAG:Dy are introduced. Finally, the effects of fluence and oxygen on temperature determination are investigated.

2. Experimental Approach

The thermographic phosphor (YAG:Dy) is deposited in powder form in an 70 µL AL_2O_3 crucible. This assembly is mounted in a precise thermal and atmospheric control stage and excited with a pulsed laser at 355 nm. An imaging spectrometer collects the phosphorescence spectra from $\lambda = 438$ to 612 nm at temperature varying from 303 K to 1773 K. Figure 1 displays the experimental setup as described below.

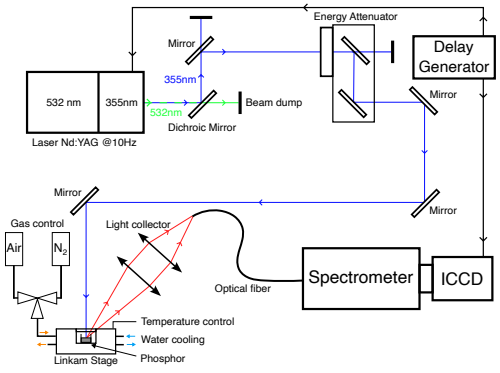

Fig. 1: Schematic diagram of the experimental set-up.

2.1. Excitation source, Laser Fluence, Temperature and Atmosphere Control

A 10 Hz pulsed Nd:YAG laser (Continuum Surelite SL II-10), of 10 ns pulse duration, operating at its third harmonic 355 nm, is used as the excitation source. To achieve laser fluences ranging from 2.5 mJ/cm^2 to 77.5 mJ/cm^2, an energy attenuator (EKSMA Optics 990-0070-355) is used to adjust the output laser energy. The laser fluence is measured following the same procedure as a previous study on the FSF method [9].

The sample is mounted on a thermal and atmospheric control stage (Linkam TS1500, S-type class 1 thermocouple), which allows temperature regulation from ambient up to 1773 K. The gas environment within the stage is controlled using a flow meter (Bronkhorst F-201CV-100-AAD-33V), delivering 60 Nml/min of Air or pure N_2 (impurity level of oxygen of 5 ppm). This setup ensures precise control over both thermal and atmospheric conditions during the acquisitions.

2.2. Phosphorescence detection and spectra acquisition

A telescope oriented at 45° of the laser path and locked on the laser beam center is used to collect the phosphorescence signal. The telescope is composed of two two-inch achromatic lenses (f_1=150 mm and f_2=100 mm, Thorlabs AC508-150-A) [9]. The sample is positioned at the focal point of the first lens to optimize data acquisition. The collected light is then focused onto a ⌀200 µm multimode optical fiber (Thorlabs TM200R5S1 A) and delivered to a spectrometer (SpectraPro-500i, 500 mm focal length, 150 grooves mm^{-1} grating, blazed at 300 nm). With a 1.5 magnification, the phosphorescence signal is collected from an elliptic surface (275 µm minor axis, 385 µm major axis) with a homogeneous laser fluence distribution, and recorded using an ICCD camera (Princeton Instruments PI-MAX4:1024f Gen III HRf, 1024×1024 resolution, 16-bit depth). The laser, the spectrometer and the camera are synchronized with an external delay generator (BNC Model 577, Pulse Generator). The spectra present in this work are calibrated not in intensity but in wavelength using a mercury lamp (INTCAL-WL-CALIB), using the *Broad auto-calibration mode* in LightField®. It yielded an RMS error of 0.073 nm. Spectra were sampled with a maximum spacing of 0.17 nm.

The camera settings are selected to maximize the signal-to-noise ratio (SNR) and prevent interference from other laser-induced emissions. The gain and the vertical hardware binning of the intensity are adjusted to ensure a Standard Error of the Mean (SEM) of less than 2% independently of the temperature and laser fluence.

The camera gate delay (GD) is chosen to be as close as possible to the end of the laser pulse to capture the most intense part of the phosphorescence spectra.

The duration of the phosphorescence signal of the YAG:Dy sample studied varies from 70 µs to 270 µs across explored temperature, laser fluence and oxygen content. However, YAG:Dy showed a short-lived broadband signal (Fig. 2), with its lifetime decreasing significantly as temperature increased [25]. Due to these broadband short-decay phosphorescence signals, the normalized phosphorescence spectra depend on the GD within the first 20 µs after the laser pulse. Therefore, a GD of 20 µs is selected for YAG:Dy and the choice of the camera gate width (GW) only impacts the SNR and not the levels of the normalized spectra.

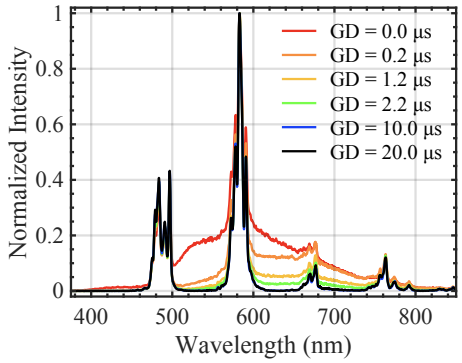

Fig. 2: Sensitivity of YAG:Dy phosphorescence spectra to gate delay at 303 K and 45 mJ/cm^2 with a gate width of 0.2 µs

For the YAG:Dy database, a gate width (GW) of 15 µs is selected to achieve the best SNR preventing the camera saturation for a sample at 303 K. This choice of GW ensures a good SNR at high temperatures as well, given the relatively small variations in intensity and phosphorescence lifetime between 303 K and 1773 K [3, 7, 15].

2.3. YAG:Dy specifications

The thermographic phosphor studied is the $Y_3Al_5O_{12}$:Dy (YAG:Dy) from Phosphor Technology (QMK66/F-X 3m/o Dy).

It is known that thermographic phosphor synthesis process have an important impact on its radiative properties which makes direct comparisons with the literature challenging [12, 26]. Thus, the YAG:Dy is characterized by X-ray Diffraction (Figure 3), using an Aeris Panalytical diffractometer working with Cu $K_{\alpha 1,2}$ wavelength in the Bragg–Brentano geometry. Diffractograms are acquired between 10° and 90° in 2-theta with a 0.02° angular step. Analysis is performed using the Profex software [27] making use of the reference phases as found in the COD database [28].

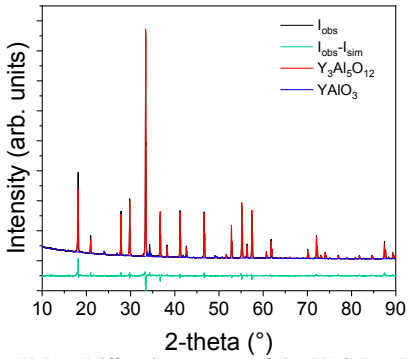

Fig. 3: X-Ray Diffraction pattern of the YAG:Dy thermographic phosphor

This analysis shows that the YAG:Dy sample mainly consists of an yttrium aluminium garnet phase $Y_3Al_5O_{12}$ (reference number cod4312142 in the COD database). The orthorhombic $YAlO_3$ parasitic phase (cod1533069, COD) is identified for $\simeq$5% of mass fraction. For both phases, the refined cell parameters i.e. a = 12.009 Å for the observed $Y_3Al_5O_{12}$ and a = 5.182 Å, b = 5.324 Å and c = 7.375 Å for the observed $YAlO_3$ are very close to the cell parameters of the original reference phases, concretely a = 12.01 Å for $Y_3Al_5O_{12}$ and a = 5.161 Å, b = 5.301 Å and c = 7.342 Å for orthorhombic $YAlO_3$.

2.4. Database acquisition

A database is constructed from the acquisitions of single-shot phosphorescence spectra of YAG:Dy during a temperature ramp of 0.4 K/s, ranging from T_{min} = 303 K to T_{max} = 1773 K, at a fixed laser fluence and a controlled oxygen concentration in the surrounding atmosphere. For each database, background acquisitions are recorded using the same temperature ramp with identical camera parameters as the signal acquisitions, under the same oxygen concentration and without laser.

Each single-shot spectrum is then corrected using the corresponding background acquisition, ensuring identical camera settings and a temperature matching within ±0.5 K as measured by the thermal stage. Every 1 K, the mean spectra are obtained by averaging 25 corrected single-shots. These mean spectra are then filtered using a third-order Savitzky–Golay smoothing filter with a 13-points moving window, and normalized to maximum intensity.

A total of 4 databases are acquired under varying laser fluences and oxygen content. Three databases are acquired in N_2 at laser fluences of F_{min} = 2.5 mJ/cm^2, F_{mid} = 42.3 mJ/cm^2 and F_{max} = 77.5 mJ/cm^2, and one database is acquired in Air at F_{max}. The database at F_{max} and N_2 will be considered as the reference database in the following.

3. FSF Method using YAG:Dy for thermometry

3.1. Method

The FSF method relies on the analysis of the dynamics of normalized spectrum from the thermographic phosphor as temperature changes. The accuracy of temperature determination critically depends on the quality of both the reference database and the acquired single-shot spectra.

With the FSF method, the computation of T_{found}, corresponding to the temperature of a phosphorescence spectrum denoted as S^{studied}, requires finding the closest match to a filtered, normalized reference spectrum. This is achieved by solving the following optimization problem:

$$\min_{T\in[\![T_{\min},T_{\max}]\!]}\{\min_{\alpha} d(\alpha S^{\text{studied}}, S_T^{\text{ref}})\} \qquad (1)$$

where $d(\cdot,\cdot)$ represents a distance metric between two spectra and α a coefficient of normalization.

This classification problem is solved using several distance metrics [29]. Among them, the L_2 distance and the Pearson χ^2 distance, which were chosen for their best performance in the case of this study, are defined as:

$$d_{L_2}(S^{\text{studied}}, S^{\text{ref}}) = \sqrt{\sum_{\lambda}\left(S_\lambda^{\text{studied}} - S_\lambda^{\text{ref}}\right)^2} \qquad (2)$$

$$d_{\text{Pearson }\chi^2}(S^{\text{studied}}, S^{\text{ref}}) = \sum_{\lambda}\frac{\left(S_\lambda^{\text{studied}} - S_\lambda^{\text{ref}}\right)^2}{S_\lambda^{\text{ref}}} \qquad (3)$$

The performance of both distance will be tested to retrieve the temperature using the FSF method on the reference database.

3.2. YAG:Dy use cases

The temperature-dependent evolution of YAG:Dy normalized phosphorescence spectra is displayed in Figure 4. Significant spectral variations are observed

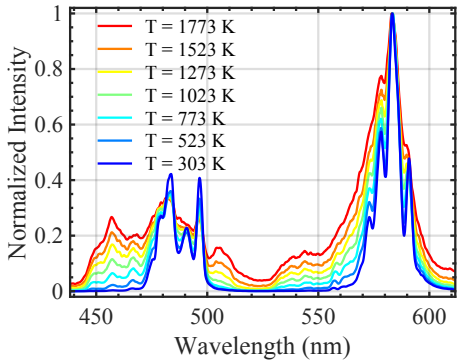

Fig. 4: Sensitivity of YAG:Dy phosphorescence spectra to temperature at F_{max} in N_2.

as a function of temperature. Although no strong variation is evident in the intensity ratio between the primary peak located around 580 nm and the secondary peaks in the 480–500 nm region of the YAG:Dy phosphorescence spectra, a more pronounced difference appears when comparing the 580 nm peak to the feature at 460 nm. The temperature sensitivity of the YAG:Dy spectrum makes this thermographic phosphor a strong candidate for the FSF method.

A cross-validation procedure with 5-folds is performed to estimate the statistical accuracy and standard deviation of the temperature deviation on the reference database: $\Delta T = T_{\text{found}} - T_{\text{recorded}}$. In this procedure, all single-shots are randomly split into five folds of approximately 5 per 1 K each. Four folds, representing approximately 20 single-shots per 1 K, are used to construct the mean-normalized spectra database, while the remaining fold serves as the test set. This process is rotated across all folds, resulting in five iterations. The estimated temperature deviation obtained from each test fold are aggregated in Figure 5. The left panel of this figure shows the evolution of the mean and standard deviation of the temperature deviations across the full temperature range. Each point corresponds to the mean and standard deviation of the deviations within ±50 K, representing roughly 2,500 single shots per point. The right panel shows the histogram of temperature deviations over the entire temperature range, with the corresponding summary statistics provided in the caption.

The histogram of Figure 5 illustrates that the Pearson χ^2 distance yields better results compared to the L_2 distance with a sub-kelvin accuracy (0.3 K) and a standard deviation below 8.4 K for the whole range of temperature studied.

In detail, the accuracy of the temperature deviation ΔT as a function of the recorded temperature remains constant around zero while the evolution of the standard deviation slightly increase with the recorded temperature. These results are of particular interest considering that, over the broad temperature range, they correspond to a remarkably low relative error. The Pearson χ^2 distance is used in the following to retrieve the temperature with the FSF method.

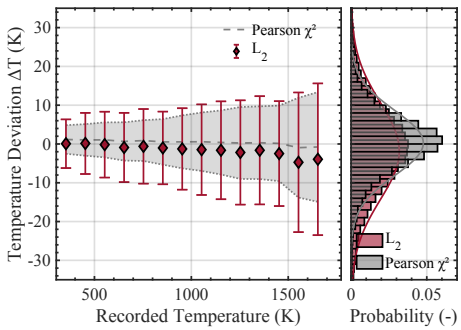

Fig. 5: Effects of distance metric on temperature deviation ΔT with the reference database at F_{max} in N_2. $\overline{\Delta T}_{L_2} = -1.8$ K, $\sigma_{\Delta T, L_2} = 12.5$ K, and $\overline{\Delta T}_{\chi^2} = 0.3$ K, $\sigma_{\Delta T, \chi^2} = 8.4$ K.

4. Laser Fluence and Oxygen Effects on Temperature determination

In combustion applications, the composition of the gas surrounding the thermographic phosphor can exhibit significant spatial and temporal fluctuations in oxygen concentration, as well as substantial laser fluence extinction (soot particules, small gaseous species, PAHs...). Ishiwada [15] and Nilsson et al. [7] have shown that oxygen concentration affects both the lifetime and intensity of YAG:Dy phosphorescence. To the authors' knowledge, only few information exists regarding the effect of oxygen concentration [15] and on the impact of laser fluence [25] on YAG:Dy normalized spectra. Characterizing these effects on normalized YAG:Dy phosphorescence spectra is essential to ensure the reliability of the FSF method.

To this end, temperature determinations of single-shot database acquired under various laser fluences and atmospheric conditions are compared against the reference database obtained at a laser fluence of F_{max} in an N_2 atmosphere.

4.1. Effect of Laser Fluence

To investigate the effect of laser fluence on the temperature determination using the FSF method, databases of single-shot spectra are acquired under N_2 atmosphere at two laser fluences F_{mid} and F_{min} respectively corresponding to a 50% and 97% extinction of the laser fluence F_{max}.

Figure 6 displays the comparison of the YAG:Dy normalized spectra for the extrema of the databases i.e. F_{min} spectra vs. F_{max} spectra at T_{min} and T_{max} with both N_2 and Air atmosphere. In this figure, the displayed spectra are obtained from the average of 250 corrected single-shot spectra. In the first column, the top graph shows two normalized spectrum obtained at F_{min} and F_{max} at temperature T_{min}. The evolution

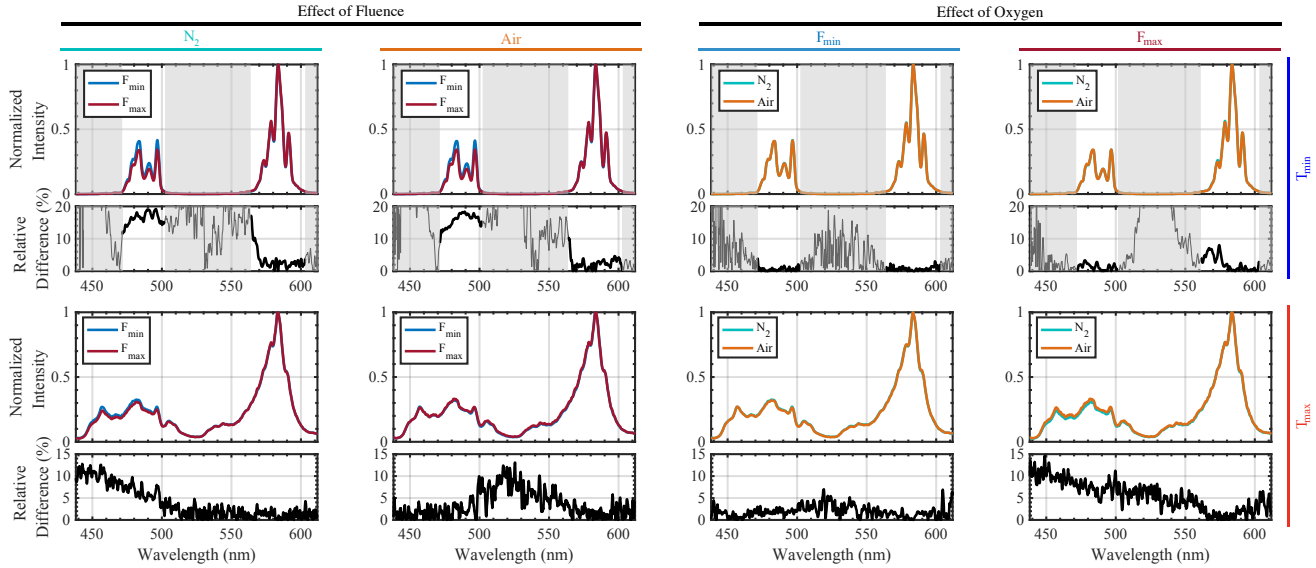

Fig. 6: Normalized intensity of the YAG:Dy phosphorescence spectrum at different conditions. Gray regions correspond to normalized intensity below 0.02. Displayed spectra are obtained from the average of 250 corrected single-shot spectra.

of the relative difference is $\geq$15% for the first spectral band 471–502 nm, and less than 5% on the second band 564–603 nm. At high temperatures, the bottom graph shows that the relative difference is about 12% at 439 nm and decreases linearly to reach 3% at 515 nm and less than 3% value throughout the rest of the spectrum. It is interesting to note that increasing temperature reduces the effect of laser fluence on the normalized spectra.

Figure 7 represents the temperature deviation ΔT between the temperature of single-shots acquired at F_{min} or F_{max} and the temperature determined by the FSF method identified using the reference database. The gray area represents the accuracy of the method as a function of temperature, as shown in Fig. 5.

The temperature deviation for single-shots at F_{min} increases with temperature, reaching $\overline{\Delta T}_{F_{min}} = 84.4$ K at $T_{F_{min}} = 1650$ K, as well as the standard deviation of $\Delta T_{F_{min}}$. As seen in the distribution of $\Delta T_{F_{min}}$ over all temperatures shown on the right of Fig. 7, the average temperature error of the FSF method is $\overline{\Delta T}_{F_{min}} = 22.5$ K in this case.

Conversely, when single-shots acquired at F_{mid} are compared to the F_{max} reference database, the absolute mean and standard deviation of the temperature deviation are comparable to those obtained using both averaged signals and single-shots from the reference database cross-validated, respectively $\overline{\Delta T}_{F_{mid}} = -2.6$ K, $\sigma_{\Delta T, F_{mid}} = 10.5$ K and $\overline{\Delta T}_{F_{max}} = 0.3$ K, $\sigma_{\Delta T, F_{max}} = 8.4$ K.

This suggests the existence of a laser fluence threshold value in the FSF method for this YAG:Dy sample. This effect was already observed in [18]. Effectively, using a database done at a laser fluence well above this threshold allows the temperature determination without any bias due to uncertainties of the laser energy.

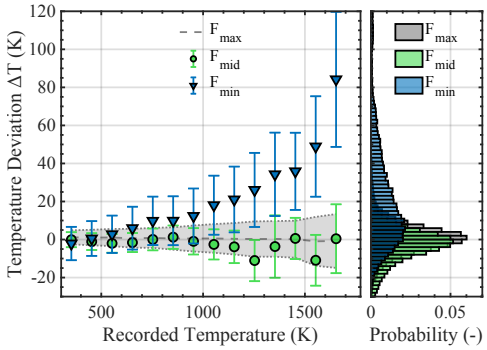

Fig. 7: Effect of laser fluence on temperature deviation ΔT. $\overline{\Delta T}_{F_{mid}} = -2.6$ K, $\sigma_{\Delta T, F_{mid}} = 10.5$ K. $\overline{\Delta T}_{F_{min}} = 22.5$ K, $\sigma_{\Delta T, F_{min}} = 28.7$ K.

4.2. Effect of Oxygen

Figure 6 displays the comparison of the YAG:Dy normalized spectra for the extrema of our databases, i.e. N_2 vs. Air atmosphere at T_{min} and T_{max} with both F_{min} and F_{max} laser fluences. At low temperatures on Figure 6, the bottom graph shows that the relative difference remains $\leq$ 8% on the first spectral band and $\leq$ 4% on the secondary spectral band. At high temperatures, the evolution of the relative difference shows a difference of around $\geq$3% on the first spectral band, and $\leq$ 15% on the secondary spectral band. The third column illustrates that at low laser fluence, the influence of oxygen concentration in the surrounding gas is negligible. Overall, these observations indicate that oxygen primarily induces minor variations in the normalized spectra of the YAG:Dy sample.

As mentioned in Sec. 4.1 the effect of oxygen concentration on the FSF method can be observed independently of the laser fluence, as long as it is greater than F_{mid}. To investigate this further, a single-shot database is collected in Air at a laser fluence of F_{max}. This data is then evaluated using a reference database

comprised of averaged single-shot spectra recorded in an N_2 atmosphere under the same laser fluence conditions. Temperature deviations obtained with the FSF method are shown in Figure 8.

Results indicate that the mean temperature deviation increases from approximately -7 K at low temperatures to -19 K at higher temperatures. Similarly, the standard deviation of the temperature deviation rises from 4 K at low temperatures to 15 K at higher temperatures.

Results indicate that the mean temperature deviation increases from approximately -7 K at low temperatures to -19 K at higher temperatures. Similarly, the standard deviation of the temperature deviation rises from 4 K at low temperatures to 15 K at higher temperatures.

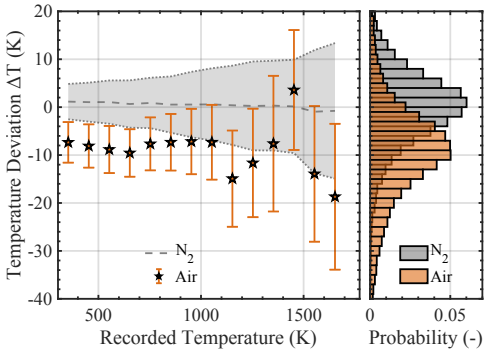

Fig. 8: Effect of oxygen on temperature deviation ΔT. $\overline{\Delta T}_{\text{Air}} = -9.6$ K, $\sigma_{\Delta T,\text{Air}} = 11.1$ K.

For air combustion system application, the uncertainty on oxygen concentration on the temperature determination by FSF method on YAG:Dy decrease acceptably the accuracy at 16 K around 1700 K and at F_{max}, which corresponds to the worst case scenario.

4.3. Guidelines for YAG:Dy FSF Method application on Combustion Chambers

This section proposes some guidelines to perform LIP measurements using YAG:Dy with FSF method in combustor.

It is important to note that the FSF method, like any other LIP thermometry method (lifetime and intensity ratio), requires prior calibration with a specific acquisition setup and a fixed thermographic phosphor sample, which must remain unchanged during temperature measurements [3]. In the case of the FSF method, the calibration consists of the creation of a database of normalized spectra for a temperature range of interest.

In the case of YAG:Dy, its normalized spectra show a dependence of laser fluence and O_2 concentration on temperature (Fig. 7 & Fig. 8). This apparent reliance necessitates the creation of multiple databases according to application needs (e.g. external or internal walls temperature measurements of a combustion chamber under rich or lean conditions). The present results indicate the existence of a threshold fluence beyond which temperature determination becomes independent of the laser fluence used for the reference database. However, in practical applications, the medium may exhibit absorption and scattering properties. Therefore, it is recommended to select a sufficiently high laser fluence to prevent potential reductions in incident energy.

Furthermore, the results show that, when using a reference database in N_2 at a laser fluence higher than the threshold, the influence of oxygen leads to a noticeable but limited difference in precision and accuracy. To minimize temperature measurement uncertainty, it is beneficial to construct a database at an oxygen concentration close to the operating conditions. For instance, in lean combustion applications, the reference database should ideally reflect the equilibrium oxygen concentration. Similarly, for rich or stoichiometric combustion conditions, it is recommended to establish a database in an N_2 environment. Moreover, it is worth mentioning that in practical application, the thermographic phosphor will be mixed with a binder, embedding it in a matrix and insulating it from the surrounding atmosphere. This could significantly reduce the influence of oxygen content.

Finally, several interference sources may arise in practice. A part from the laser extinction mentioned above, another one is spectral absorption of emitted light by media like H_2O or CO_2, though this mainly affects the infrared and has minimal impact in the visible range used here. In combustion chambers, absorption can be further reduced, for example by applying the thermographic phosphors to quartz windows to avoid and/or minimize optical path through absorbing gases. Flame emissions may also interfere from several sources. Spontaneous emissions from radicals such as OH* and CH* are commonly observed, but since they lie outside our spectral region of interest, they would not interfere. In very fuel-rich hydrocarbon flames, however, emissions from species like C_2 or C_3 may overlap with the visible range of interest. In such cases, their impact can be reduced by ignoring the corresponding spectral bands, for instance by applying masks during data processing. Furthermore, when measurements are performed under stationary conditions, background subtraction further limits the influence of these spontaneous emissions. Laser excitation can also stimulate emissions, notably from OH and CH radicals. Nevertheless, these emissions do not significantly affect the measurements, as their fluorescence lifetimes are very short (on the order of 400–600 ns [30, 31]) compared to the system's gating, making their contribution negligible. Another source of interference comes from continuous spectral emissions. Thermal radiation in the infrared can be strong but typically falls outside the spectral window of interest. By contrast, soot can emit strongly in the visible range and may disturb the measurement. When this occurs in steady conditions, its contribution can also be effectively minimized by subtracting the background.

5. Conclusion

This study investigated the spectral dynamics of YAG:Dy phosphorescence signals with varying temperatures for thermometry applications using the FSF method. The method was successfully employed over a wide temperature range from 303 K to 1773 K.

Over the studied temperature range, YAG:Dy exhibits a strong spectral dependence, making it advantageous over lifetime-based methods below 1200 K.

An improved signal processing approach was proposed by selecting a more effective spectral distance metric, Pearson χ^2 distance, which resulted in better temperature determination accuracy. At a given operating point, using an appropriate distance metric and minimization method, the deviation between the recorded and found temperature remained sub-kelvin on average, with a standard deviation of 8.4 K.

For combustion chamber applications, laser fluence can be affected by the presence of UV semi-transparent gases and by fluctuations in oxygen levels in gases. The sensitivity to these factors of YAG:Dy phosphorescence spectra, applied to the FSF method, was evaluated under different operating conditions.

The results indicate that YAG:Dy is sensitive to laser fluence, especially at low laser fluences, but there is a threshold above which the temperature determined by the FSF method is no longer affected by variations in laser fluence.

The presence of oxygen affects the response of the phosphor, but its influence is limited. The relative error remains below 1.5% across the entire measurement range, even under conditions of high laser fluence and high temperature, where the effects are most noticeable.

The study concludes with practical guidelines for implementing the FSF method in combustion chambers. To minimize sensitivity to both laser fluence and oxygen concentration, a balanced approach is required. Maximizing laser fluence improves the signal-to-noise ratio and mitigates the sensitivity observed at low laser fluence levels. However, laser fluence should not be excessively high to avoid additional variability cause by fluctuations in oxygen content.

Future work will extend this analysis to YAG:Dy mixed with a binder, aiming to study the sensitivity of this mixture to fluence and oxygen levels. Additionally, applications in combustion chambers will be explored.

Declaration of competing interest

The author declares that they have no known competing financial interests or personal relationships that could have appeared to influence the work reported in this paper.

Acknowledgement

This study was conducted as part of the HyMaX and OXY3C projects, both funded by the French National Research Agency under the projects "ANR-23-CD50-0021-01" and France 2030 program, reference "ANR-22-PESP-0009", respectively.

This work also received financial support from the LabEx LaSIPS (ANR-10-LABX-0032-LaSIPS), managed by the French National Research Agency under the "Investissements d'Avenir" program (ANR-11-IDEX-0003-02).

References

[1] A. Degenève, P. Jourdaine, C. Mirat, J. Caudal, R. Vicquelin, T. Schuller, Analysis of wall temperature and heat flux distributions in a swirled combustor powered by a methane-air and a CO_2-diluted oxyflame, Fuel 236 (2019) 1540–1547.

[2] A. H. Khalid, K. Kontis, Thermographic phosphors for high temperature measurements: principles, current state of the art and recent applications, Sensors 8 (9) (2008) 5673–5744.

[3] J. Brübach, C. Pflitsch, A. Dreizler, B. Atakan, On surface temperature measurements with thermographic phosphors: a review, Progress in Energy and Combustion Science 39 (1) (2013) 37–60.

[4] A. O. Ojo, D. Escofet-Martin, B. Peterson, High-precision 2D surface phosphor thermometry at kHz-rates during flame-wall interaction in narrow passages, Proceedings of the Combustion Institute 39 (1) (2023) 1455–1463.

[5] A. Mendieta, B. Fond, P. Dragomirov, F. Beyrau, A delayed gating approach for interference-free ratio-based phosphor thermometry, Measurement Science and Technology 30 (7) (2019) 074002.

[6] Y. Wu, Y. Zhang, T. Fu, Y. Du, L. Zhou, Y. Zhang, Measurements of blade temperature distribution in engine combustion environments using two-color luminescence imaging thermometry based on atmospheric-plasma-sprayed YAG:Dy coatings, Applied Physics B 131 (4) (2025) 91.

[7] S. Nilsson, H. Feuk, M. Richter, High temperature thermographic phosphors YAG: Tm; Li and YAG: Dy in reduced oxygen environments, Journal of Luminescence 256 (2023) 119645.

[8] S. Petit, P. Xavier, G. Godard, F. Grisch, Improving the temperature uncertainty of Mg4FGeO6:Mn4+ ratio-based phosphor thermometry by using a multi-objective optimization procedure, Applied Physics B 128 (3) (2022) 57.

[9] V. Lechner, C. Betrancourt, C. Mirat, P. Scouflaire, S. Ducruix, Full spectrum fitting method: a new approach for instantaneous phosphor thermometry in harsh environments, Experiments in Fluids 63 (7) (2022) 110.

[10] V. Lechner, C. Betrancourt, P. Scouflaire, L. Vingert, S. Ducruix, Dynamic characterization of wall temperature in LOX/CH_4 rocket engine operating conditions using phosphor thermometry, Proceedings of the combustion institute 39 (4) (2023) 5033–5041.

[11] J. Feist, A. Heyes, S. Seefeldt, Oxygen quenching of phosphorescence from thermographic phosphors, Measurement Science and Technology 14 (5) (2003) N17.

[12] J. Brübach, A. Dreizler, J. Janicka, Gas compositional and pressure effects on thermographic phosphor thermometry, Measurement Science and Technology 18 (3) (2007) 764.
[13] T. Kissel, J. Brübach, M. Euler, M. Frotscher, C. Litterscheid, B. Albert, A. Dreizler, Phosphor thermometry: On the synthesis and characterisation of Y3Al5O12: Eu (YAG: Eu) and YAlO3: Eu (YAP: Eu), Materials Chemistry and Physics 140 (2-3) (2013) 435–440.
[14] L. Yang, D. Peng, X. Shan, F. Guo, Y. Liu, X. Zhao, P. Xiao, "oxygen quenching" in eu-based thermographic phosphors: mechanism and potential application in oxygen/pressure sensing, Sensors and Actuators B: Chemical 254 (2018) 578–587.
[15] N. Ishiwada, K. Tsuchiya, T. Yokomori, Applicability of dy-doped yttrium aluminum garnet (YAG:Dy) in phosphor thermometry at different oxygen concentrations, Journal of Luminescence 208 (2019) 82–88.
[16] J. Brübach, J. Feist, A. Dreizler, Characterization of manganese-activated magnesium fluorogermanate with regards to thermographic phosphor thermometry, Measurement Science and Technology 19 (2) (2008) 025602.
[17] C. Abram, B. Fond, F. Beyrau, High-precision flow temperature imaging using zno thermographic phosphor tracer particles, Optics express 23 (15) (2015) 19453–19468.
[18] E. Hertle, S. Will, L. Zigan, Characterization of yag: Dy, er for thermographic particle image velocimetry in a calibration cell, Measurement Science and Technology 28 (2) (2017) 025013.
[19] J. Feist, A. Heyes, K. Choy, B. Su, Phosphor thermometry for high temperature gas turbine applications, in: ICIASF 99. 18th International Congress on Instrumentation in Aerospace Simulation Facilities. Record (Cat. No.99CH37025), IEEE, 1999, pp. 6/1–6/7.
[20] M. Cates, YAG:Dy and YAG:Tm fluorescence above 1400 c., Tech. rep., Oak Ridge National Lab.(ORNL), Oak Ridge, TN (United States) (2003).
[21] M. Yu, G. Särner, C. Luijten, M. Richter, M. Aldén, R. Baert, L. De Goey, Survivability of thermographic phosphors (YAG:Dy) in a combustion environment, Measurement science and technology 21 (3) (2010) 037002.
[22] J. Eldridge, T. Jenkins, S. Allison, D. Wolfe, E. Jordan, Development of YAG:Dy thermographic phosphor coatings for turbine engine applications, in: 58th International Instrumentation Symposium, no. E-18445, 2012.
[23] S. Allison, D. Beshears, M. Cates, M. Scudiere, D. Shaw, A. Ellis, Luminescence of YAG:Dy and YAG:Dy, Er crystals to 1700° c, Measurement Science and Technology 31 (4) (2020) 044001.
[24] J. Feist, A. Heyes, S. Seefeldt, Thermographic phosphors for gas turbines: instrumentation development and measurement uncertainties 11th int, in: Symp. on Application of Laser Techniques to Fluid Mechanics (Lisbon, Portugal, 2002.
[25] M. Lawrence, H. Zhao, L. Ganippa, Gas phase thermometry of hot turbulent jets using laser induced phosphorescence, Optics express 21 (10) (2013) 12260–12281.
[26] S. N. Ogugua, C. Abram, B. Fond, R. E. Kroon, F. Beyrau, H. C. Swart, Effect of annealing conditions on the luminescence properties and thermometric performance of $Sr_3\ Al_2\ O_5\ Cl_2$:Eu^{2+} and $SrAl_2\ O_4$:Eu^{2+} phosphors, Dalton Transactions 53 (10) (2024) 4551–4563.
[27] N. Doebelin, R. Kleeberg, Profex: a graphical user interface for the rietveld refinement program bgmn, Applied Crystallography 48 (5) (2015) 1573–1580.
[28] S. Gražulis, A. Daškevič, A. Merkys, D. Chateigner, L. Lutterotti, M. Quiros, N. R. Serebryanaya, P. Moeck, R. T. Downs, A. Le Bail, Crystallography open database (cod): an open-access collection of crystal structures and platform for world-wide collaboration, Nucleic acids research 40 (D1) (2012) D420–D427.
[29] S.-H. Cha, Comprehensive survey on distance/similarity measures between probability density functions, City 1 (2) (2007) 1.
[30] K. H. Becker, H. H. Brenig, T. Tatarczyk, Lifetime measurements on electronically excited Ch(A2) radicals, Chemical Physics Letters 71 (2) (1980) 242–245.
[31] C. W. Bauschlicher, S. R. Langhoff, Theoretical determination of the radiative lifetime of the A 2+ state of OH, The Journal of Chemical Physics 87 (8) (1987) 4665–4672.